18th Australasian Fluid Mechanics Conference
Launceston, Australia
3-7 December 2012

Computational Stability Analysis of a Channel Flow with a Large Deformation Compliant Insert

L.S.H. Lai[1], A.D. Lucey[1] and N.S.J. Elliott[1]

[1]Fluid Dynamics Research Group
Curtin University, Perth, Western Australia 6845, Australia

Abstract

We consider a fluid-conveying channel with a compliant insert, or wall, undergoing flow-induced deformations. The objective is to understand the mechanism that can cause self-excited oscillations of a fundamental system that underpins a host of both engineered (e.g. flexible-pipes, membrane filters) and biomechanical (e.g. blood flow, airway flow) applications. The computational model is developed using the open-source fluid-structure interaction software `oomph-lib` that accounts for unsteady laminar flow interacting with large-amplitude deformations of a thin flexible wall. The fluid loading on the compliant wall comprises both pressure and viscous stresses while the wall mechanics includes flexural and tensile forces. The discretised equations for the coupled fluid and structural dynamics are combined to yield a single monolithic matrix differential equation for fluid and wall variables, which is solved through a time-stepping procedure. We present a brief summary of validations performed that demonstrate the appropriateness of `oomph-lib` as a modelling tool for the system. Cases are then presented to contrast the system in stable and unstable conditions and we offer an explanation of the physical causes of non-linear saturated oscillation by examining the nature of wall deformations and their effect on the pressure gradient along the wall. We surmise that instability occurs principally through fluctuating energy transfers between wall and fluid that are driven by separation-point changes over each cycle of oscillation.

Introduction

The occurrence of flutter of a fluid-conveying flexible pipe with fixed ends is a significant fundamental phenomenon. It has many biomechanical applications because flexible conduits are common in the human body; examples of these are arterial, venous, lymphatic, pulmonary airway and urinary systems [1]. The dynamics of fluid-conveying flexible pipes have been comprehensively studied through laboratory experiments using the Starling Resistor paradigm; for example see [2]. Modelling of the system dynamics was first undertaken by Pedley [3], using the simplified two-dimensional analogue model of Figure 1 that consists of a 2-dimensional (2-d) channel with one segment of the wall replaced by a membrane under longitudinal tension. This remains an important model because it avoids the complications of the fully 3-d flow found in the Starling Resistor while exhibiting flow limitation and self-excited oscillations [4]. Significant progress has been made towards understanding the complex stability characteristics of this simplified model, especially through the recent numerical work of Luo & Pedley [5, 6, 7] using an in-house code.

The present paper outlines a complementary approach that uses the open-source object-oriented multiphysics finite element library `oomph-lib` [8]. Liu *et al.* [9] show that the system dynamics can be sensitive to the modelling adopted. Our approach then offers a further independent assessment of this variability. In addition, the access and versatility provided by `oomph-lib` permits us to conduct investigations of the causes of self-excited oscillations. Thus, the main contribution of this paper is to highlight, by contrasting two typical cases, one stable and the other unstable, the principal phenomena that underlie the mechanism of self-excited oscillations in the system.

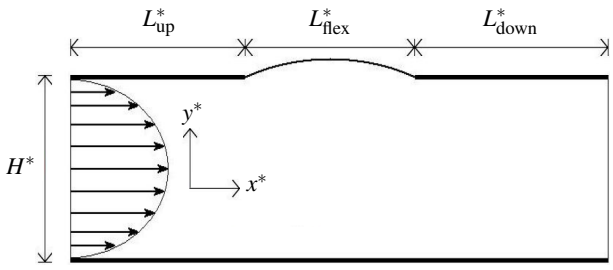

Figure 1: Geometry of the 2-d channel with complaint insert

Theoretical and Computational Modelling

Figure 1 shows the major geometrical parameters of the model. Variables identified with asterisks are dimensional and those without are nondimensional. Fluid flow is driven by a prescribed Poiseuille velocity profile at the inlet of the 2-d channel of width H^*, the characteristic length used for nondimensionalisation, and total length L^*_{total}; the channel Eulerian coordinates (x^*,y^*) have their origin at the lower left corner of the channel. The total length is the sum of the upstream length L^*_{up}, flexible section length L^*_{flex}, and downstream length L^*_{down}. The upstream and downstream sections are rigid, and the central section is an elastic plate hinged at both ends.

We now provide only a brief summary of the governing equations because the general formulation is provided in [4]. Its application to the specific problem at hand is in our previous work [10, 11] wherein it is seen that, for a given wall geometry, the non-dimensional solution space is governed by two parameters. These are the Reynolds number, $\text{Re} = \rho^* U^*_{\text{mean}} H^* / \mu^*$, and the ratio of viscous-fluid to elastic-solid stresses, $Q = [\mu^* U^*_{\text{mean}} / H^*] / E^*_{\text{eff}}$, in which ρ^*, U^*_{mean} and μ^* are respectively the fluid density, mean flow speed (at entry) and dynamic viscosity, while E^*_{eff} is the effective (accounting for Poisson ratio) elastic modulus.

The Newtonian fluid is governed by the incompressible Navier-Stokes equations and continuity equation. The boundary conditions are that the inflow has a plane Poiseuille velocity profile (with mean speed U^*_{mean}) and no slip is enforced on both rigid and flexible walls. The pressure at the outlet is set to zero and this serves as the datum for the applied external pressure, P^*_{ext}, and the pressure perturbation added to this to initiate motion of the wall.

The beam deformation is governed by the nondimensional form of the principle of virtual displacements.

The wall is loaded by an external pressure P_{ext} and the traction that the fluid exerts on it. The components of load vector f that

act on the wall are given by

$$f_{\rm i} = -P_{\rm ext}N_{\rm i} + Q\left(pN_{\rm i} - \left(\frac{\partial u_{\rm i}}{\partial x_{\rm j}} + \frac{\partial u_{\rm j}}{\partial x_{\rm i}}\right)N_{\rm j}\right), \qquad (1)$$

for $i, j = 1, 2$, where $N_{\rm i}$ are the Eulerian components of the outer unit normal on the boundary of the fluid domain. Q quantifies the strength of the fluid-structure interaction (FSI).

Numerical Implementation

The solution procedure is formulated using `oomph-lib`. Two-node Hermite beam elements are used for the Kirchoff-Love 1-d beam, which are geometrically nonlinear with incrementally linear constitutive equations, while nine-node quadrilateral Taylor-Hood elements are used for the fluid. Nodal positions are updated in response to the changes in the flexible-wall position as it deforms. Time-stepping is performed using a Newmark scheme for the solid and a backward difference scheme for the fluid. The solid and fluid components are assembled into a monolithic nonlinear FSI system equation that is solved using the Newton-Raphson method, employing the SuperLU direct linear solver within the Newton iteration.

Startup Procedure

A fully-developed viscous flow passes through the channel at the start of a simulation by specifying the mean inlet velocity $U_{\rm inlet}$. Linearly varying external pressure is then applied to negate the pressure due to the fluid flow and thus maintain the wall in the as-undeformed state. This external pressure is then gradually removed whilst two new uniform external pressures are applied. The first, $P_{\rm ext}$, is applied to give the flexible wall a deformed mean shape. The second is a perturbation pressure, $P_{\rm pturb}$, to excite the system. After a small number of time-steps $P_{\rm pturb}$ is removed and the system becomes unsteady.

Parameter Values

The system parameters for the two cases addressed in this paper are given in Table 1. The dimensional quantities give an appreciation of the physical scales of the problem; the non-dimensional quantities characterise the mean amplitude of the FSI-based wall deformation. These were chosen to align exactly with the simulations of Cases A and C in the study of Liu *et al*. [9] as a validation exercise for the present model. Herein, we refer to these as Case I and Case II that respectively characterise stable and unstable behaviours about the mean wall deformation. Both cases comprise a water-like fluid density flowing past a rubber-type flexible wall that has no pre-stress. We use a massless (zero density) flexible wall, our previous work having shown that under these conditions the wall inertia is negligible compared to that of the fluid.

Table 1: Dimensional (upper) and non-dimensional control (lower) parameter values for the two cases studied

Parameter	Value	
	Case I (Unstable)	Case II (Stable)
$L^*_{\rm up}$ (mm)	50	50
$L^*_{\rm flex}$ (mm)	50	50
$L^*_{\rm down}$ (mm)	300	300
H^* (mm)	10	10
h^* (mm)	0.1251	0.1254
ρ^*_f ($\times 10^3$ kg/m^3)	1	1
μ^* ($\times 10^{-3}$ Pa.s)	1	1
$U^*_{\rm inlet}$ ($\times 10^{-2}$ m/s)	3	5
B^* ($\times 10^{-9}$N.m)	1.6292	78.62
$P^*_{\rm ext}$ (Pa)	-4.255	-4.875
$P_{\rm pturb^*}$ ($\times 10^{-2}$ Pa)	50	15.8
Re	300	500
Q ($\times 10^{-7}$)	2.9986	0.1045

Results

Figures 2a and 2b respectively show the wall profile, y ($= y^*/H^*$), and the pressure distribution, p ($= p^*/[\mu^* U^*/H^*]$), along the wall for the equilibrium states that arise for Cases I and II prior to a perturbation being applied. Despite its higher flow speed (Re), the much lower value of Q — that can be interpreted as the ratio of the fluid loading to wall stiffness — in Case II results in both a much lower wall-deflection amplitude and a mode shape similar to that of the wall's in-vacuo fundamental mode, as compared with Case I. Significantly, this yields a far milder adverse pressure gradient downstream of the peak amplitude and the absence of flow separation in Fig. 2b. By contrast Case I evidences an extreme pressure gradient with (steady) separation occurring at approximately $x = 9.3$. Applying a perturbation to these equilibria leads to the time series seen in Fig. 3. Oscillations are quickly attenuated in Case II. In contrast, Case I exhibits evolving transient oscillations that evolve into sustained self-excited limit-cycle oscillations after approximately $t = 150$. These results indicate that flow separation must be implicated in the mechanism of sustained oscillations. We also remark that these time series evidence excellent agreement with the ADINA-modelling results presented in [9]. It also serves to validate the present model along with our previous extensive validations of the system's component parts [10, 11].

We now focus on the details of Case I in order to elucidate the physics of its sustained self-excited oscillations by investigating one cycle of oscillation, $t : 193.2 \rightarrow 200.7$, in Fig. 3. Figures 4a and 4b respectively show snap-shots of the flexible-wall profile and the fluid pressure along the profile for a sequence of equally-separated times through the cycle; also included in these figures are the equilibrium values for Case I presented in Figs. 2a and 2b. Figure 5 shows the instantaneous flow fields for the same cycle and at the same times. In Fig. 4a, the change in wall length corresponds to the variation (about its steady equilibrium value) of the wall force through the cycle given that this is dominated by induced tension for the physical properties used herein. At its smallest amplitude in the cycle, the external pressure, combined with a reduced internal pressure on the upstream face of the deformation, act to restore the wall to its equilibrium position. At the largest amplitude it is the wall tension combined with an increased internal pressure on the upstream face that provides a net force returning the wall to the equilibrium position. Accordingly, a system of forcing that permits oscillatory behaviour is set up. However, this in itself does not explain the sustained oscillations given that the FSI system is dissipative through viscous effects in the fluid. There must therefore be an energy-exchange mechanism between the wall and the fluid flow that has a continuous upstream supply of kinetic energy and a means of convecting out energy from the site of the FSI.

Figure 6 therefore presents the time variation of the rate of energy transfer to/from the wall by the fluid flow for each of its four quartiles. This is obtained by summing the scalar product of the pressure force and the wall velocity over the length of each quartile. We do not need to consider the corresponding rate

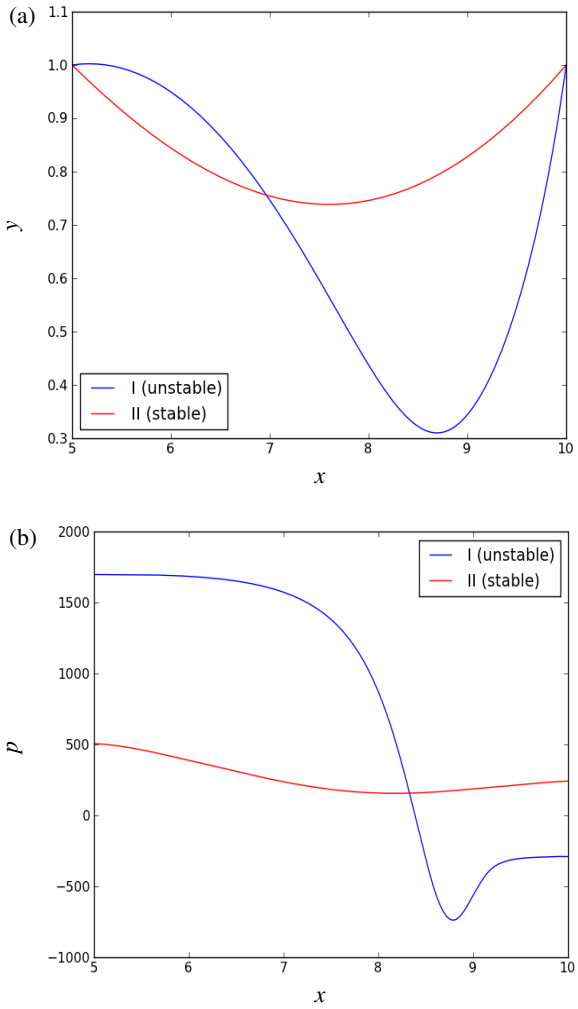

Figure 2: (a) Profile of and (b) pressure distribution along the flexible wall in the steady state.

of work against the external pressure because this force does not provide a means of irreversible energy transfer; it can be considered analogous to an external spring backing to the wall. We first remark that the addition of the four traces — a sum over the entire wall — in Fig. 6 (dashed line) yields a periodic signal with zero time average because there cannot be net energy transfer to the wall in a limit-cycle oscillation. However, there is a periodic fluctuation of energy transfer between wall and fluid and the greatest component of this arises from the fourth quartile that includes the flow-separation zone. Here, for motion in the cycle when the wall amplitude exceeds that of the steady equilibrium position, it is from wall to fluid while an equivalent and opposite energy flow occurs in the other half of the cycle. Inspection of Fig. 4b suggests that this cyclical energy flow is caused by the fore and aft variation of the separation point from that in the steady equilibrium state.

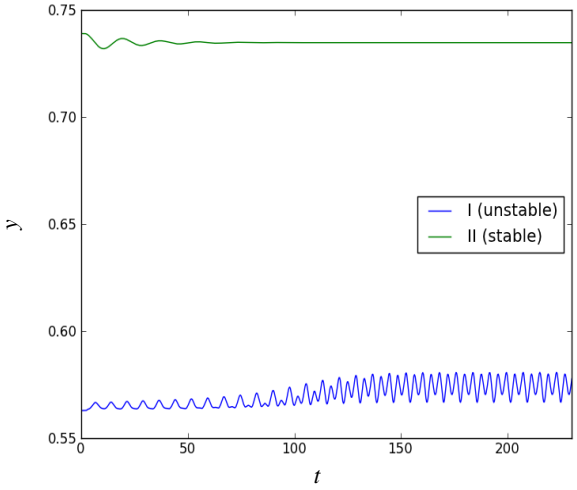

Figure 3: Oscillation of the flexible wall midpoint.

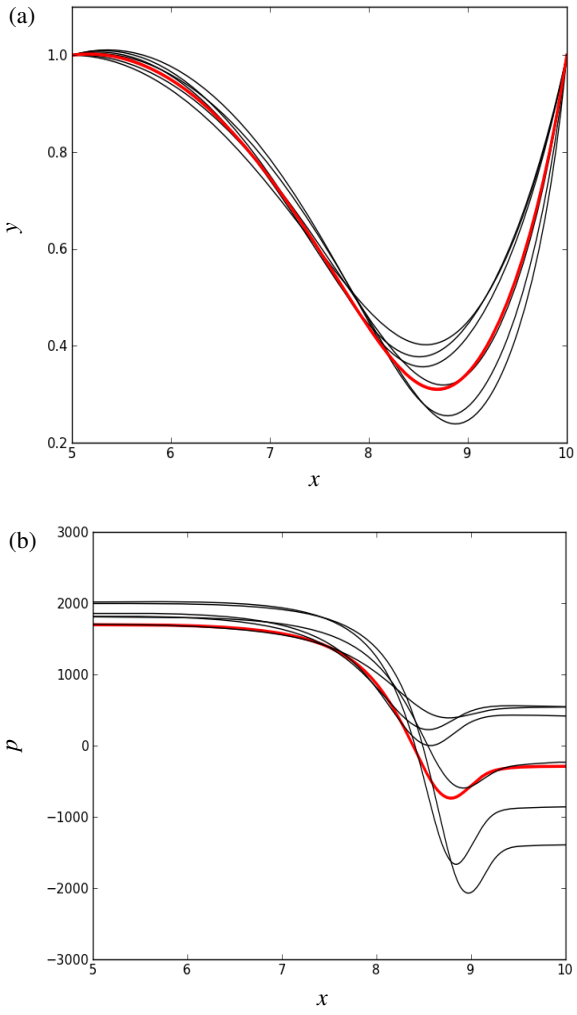

Figure 4: The variation in (a) wall profile and (b) fluid pressure along the flexible wall during one oscillation cycle.

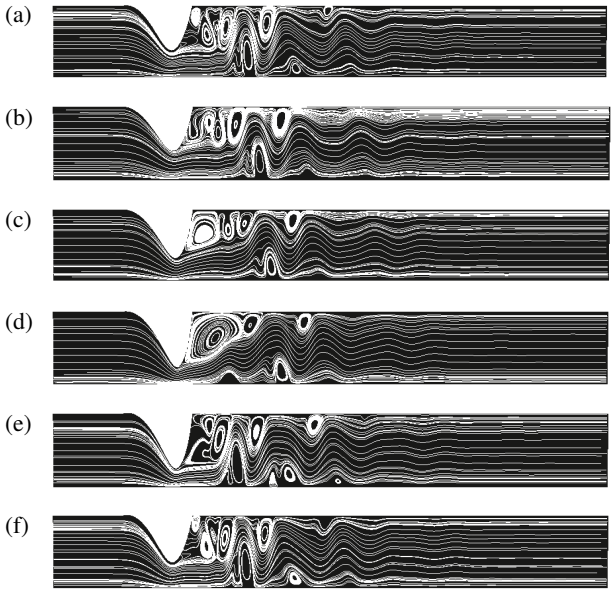

Figure 5: Fluid streamlines over one oscillation cycle; (a) t=193.2, (b) t=194.7, (c) t=196.2, (d) t=197.7, (e) t=199.2, (f) t=200.7.

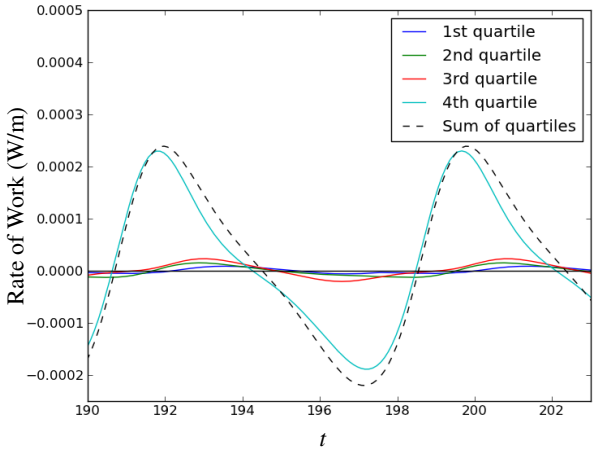

Figure 6: Rate of work in quartiles of the flexible wall for one oscillation.

Conclusions

We have presented a computational model of unsteady laminar flow in a plane channel interacting with a compliant wall replacing a section of one side of the channel and used this to investigate the sustained self-excited oscillations that are found to occur about a large-amplitude deformed-wall state. Our findings suggest that the cyclical variation of the flow-separation point is the main cause of fluctuating energy transfers between wall and flow that permit the limit-cycle oscillations of the flexible wall to exist.

Acknowledgements

The authors would like to acknowledge the development of `oomph-lib` at the School of Mathematics, University of Manchester. We would also like to thank the Australian Government through the Australian Postgraduate Awards (APA), Curtin University and the Society for Underwater Technology for their financial support.

References

[1] Bertram, C.D. 2009, Fluid Flow in Distensible Vessels, *Clinical and Experimental Pharmacology and Physiology*, **36**, 2009, 206–216.

[2] Dodds, H.L. and Runyan, H.L., Effect of High-Velocity Fluid Flow on the Bending Vibrations and Static Divergence of a Simply Supported Pipe, *NASA Technical Note*, **NASA TN D-2870**, 1965.

[3] Pedley, T.J., Longitudinal Tension Variation in Collapsible Channels: A Mechanism for the Breakdown of Steady Flow, *ASME Journal of Biomechanical Engineering*, **114**, 1992, 60–67.

[4] Heil, M. and Jensen, O.E., Flows in Deformable Tubes and Channels Theoretical Models and Biological Applications, *Fluid Mechanics and Its Applications*, **72**, 2003, 15–50.

[5] Luo, X.Y. and Pedley, T.J., A numerical simulation of unsteady flow in a two-dimensional collapsible channel, *Journal of Fluid Mechanics*, **314**, 1996, 191–225.

[6] Luo, X.Y., Cai, Z.X., Li, W.G. and Pedley, T.J., The cascade structure of linear instability in collapsible channel flows, *Journal of Fluid Mechanics*, **600**, 2008, 45–76.

[7] Liu, H.F., Luo, X.Y. and Cai, Z.X., Stability and energy budget of pressure-driven collapsible channel flows, *Journal of Fluid Mechanics*, **705**, 2012, 348–370.

[8] Heil, M. and Hazel, A., Oomph-lib An Object-Oriented Multi-Physics Finite-Element Library, *Fluid-Structure Interaction*, Springer, 2006, 19–49.

[9] Liu, H.F., Luo, X.Y., Cai, Z.X. and Pedley, T.J., Sensitivity of Unsteady Collapsible Channel Flows to Modelling Assumptions, *Communications in Numerical Methods in Engineering*, **25**, Wiley Online Library, 2009, 483–504.

[10] Lai, L., Elliott, N.S.J., Lucey, A.D. and Pitman, M.W., Numerical Two-dimensional Flexible Channel Model Fixed at Both Ends for Flow-Induced Instability Analysis, *Proc. 6th Australasian Congress on Applied Mechanics*, Engineers Australia, 2010, 207–211.

[11] Lai, L., Elliott, N.S.J., Lucey, A.D. and Pitman, M.W., Computational Modelling of a Fluid-Conveying Flexible Channel Using oomph-lib, *Proc. 19th International Congress on Modelling and Simulation*, 2011.

[12] Elliott, N.S.J., Lucey, A.D. and Heil, M., Large-Amplitude Oscillations of a Finite-Thickness Cantilevered Flexible Plate in Viscous Channel Flow, *Proc. ASME FEDSIM-ICNMM2010-30438*, 2010.